

Effect of energetic ions on plasma damage of porous SiCOH low-*k* materials

E. Kunnen, M. R. Baklanov,^{a)} A. Franquet, D. Shamiryanyan, T. V. Rakhimova,^{b)}
A. M. Urbanowicz,^{c)} H. Struyf, and W. Boullart
Imec, Heverlee, B-3001 Leuven, Belgium

(Received 12 August 2009; accepted 2 March 2010; published 19 April 2010)

Plasma damage of SiCOH low-*k* films in an oxygen plasma is studied using a transformer coupled plasma reactor. The concentration of oxygen atoms and O₂⁺ ions is varied by using three different conditions: (1) bottom power only, (2) bottom and top power, and (3) top power only. After plasma exposure, the low-*k* samples are characterized by various experimental techniques. It is shown that the ion bombardment induced by the bottom power minimizes the plasma damage by increasing the recombination coefficient of oxygen radicals. Contrary to the expectations, the densification of the top surface by ion radiation was limited. The increase in the recombination coefficient is mainly provided by modification of the pore wall surface and creation of chemically active sites stimulating the recombination of oxygen atoms. The results show that a reduction in plasma damage can be achieved without sealing of low-*k* top surface. © 2010 American Vacuum Society.
[DOI: 10.1116/1.3372838]

I. INTRODUCTION

Scaling in the ultralarge scale integration (ULSI) industry drives the distances between interconnects to dimensions where capacitance between adjacent lines starts to play a critical role. New materials providing lower capacitance values, so called low dielectric constant (low-*k*) materials, have been extensively studied during the past 10 years. In the integration process, these low-*k* materials are exposed to etch and strip plasmas. Presently popular porous plasma enhanced chemical vapor deposition (PECVD) carbon doped silica (SiCOH) materials have a hybrid nature: Organic hydrophobic groups can be removed during the exposure in oxygen and hydrogen based plasmas used for strip and postetch cleaning purposes. As a result, the matrix of these low-*k* materials becomes SiO₂-like and hydrophilic. The subsequent moisture adsorption drastically increases their dielectric constant and deteriorates reliability of integrated structures. Such degradation of low-*k* materials is termed as “plasma damage.”¹⁻⁹

Plasma damage is a complex phenomenon that depends on different plasma components such as active radicals, vacuum ultraviolet (VUV) photons, and ion irradiation. Degree and depth of plasma damage also depend on the materials properties.¹⁰ The most critical ones are related to porosity, pore size, and connectivity.^{1,2} For instance, in the case of radicals based technology (downstream plasma) the depth of damage is defined by the penetration depth of active radicals, which mainly depends of their recombination probability on the pore wall.^{11,12} In the presence of ion bombardment and in the case of a highly polymerizing carbon based plasma, the penetration of active radicals and degree of damage can be

reduced by densification of the top surface and pore sealing by fluorocarbon polymers.^{1,13,14} The impact of the plasma damage increases with downscaling of the wiring pitch because the feature size is becoming comparable to the depth of radical penetration. Therefore, fundamental understanding of plasma damage mechanisms is extremely important for the development of damage free processes. This is the reason why significant efforts by researchers are presently oriented to a separate study of VUV photons, energetic ions, and radicals impact on plasma damage of low-*k* materials.¹⁵⁻¹⁸ Although quite significant understanding of different factors has been achieved, the studies in the references are based on special tools and instrumentations.

In this work, the effect of an oxygen plasma on a porous SiCOH films is studied in a commercially available transformer coupled plasma (TCP) reactor. Such reactors are widely used in ULSI technology for etch and *in situ* strip purposes. TCP reactors offer the advantage of having a reasonably separated control between radical concentration and ion bombardment (Fig. 1). An oxygen plasma was used as a model system because the degree of low-*k* damage is more pronounced in comparison with H₂ based plasmas. However, in some cases, an oxygen plasma causes less damage in comparison with N₂/H₂ plasmas.^{19,20} The reason why this more aggressive plasma can generate less damage in some cases does not have any reasonable explanation so far.

For revealing the interaction mechanisms, three conditions, allowing a controllable change in intensity of ion irradiation and radicals concentration are investigated: (1) bottom power only (BPO), (2) top and bottom powers (T&BP) at the same time, and (3) top power only (TPO). By this way, we were able to change the plasma condition from a pure capacitively coupled regime (BPO) to inductive plasma conditions (TPO) with reduced energy of ion bombardment. After exposure, the low-*k* samples are characterized by different techniques: spectroscopic ellipsometry (SE) was used to

^{a)}Electronic mail: baklanov@imec.be

^{b)}Present address: Skobeltsyn Institute of Nuclear Physics, Lomonosov Moscow State University, Moscow, Russia.

^{c)}Also at Chemistry Department, Katholieke Universiteit Leuven, Heverlee, Belgium.

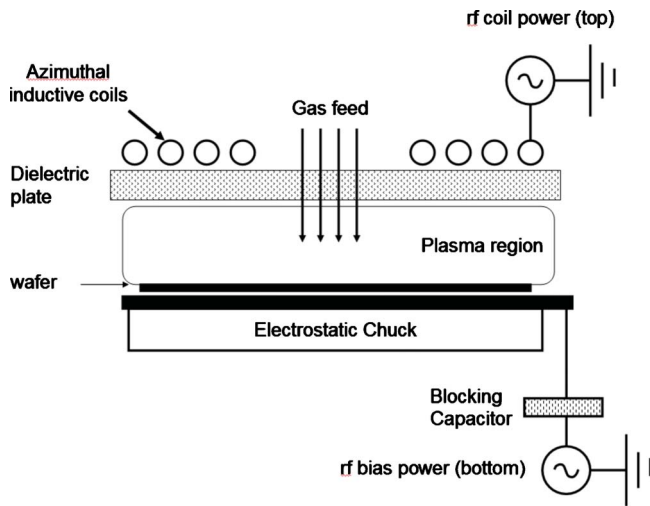


FIG. 1. (Color online) TCP plasma reactor layout.

evaluate the change and gradient of optical characteristics and surface densification; ellipsometric porosimetry (EP) to evaluate porosity, pore size, and pores sealing (toluene based EP) and degree of hydrophilization of internal pore surface (water-based EP); water contact angle (WCA) to evaluate surface hydrophilization; Fourier transformed infrared spectroscopy (FTIR) to evaluate change in chemical composition; energy filtered transmission electron microscopy (EFTEM) and time of flight secondary ion mass spectrometry (TOF SIMS) to evaluate the depth of chemical modification. The combination of these techniques allows obtaining key information related to plasma damage: change in chemical composition, densification, and hydrophilization of the damaged layer.

It is found that the difference between BPO, T&BP, and TPO conditions is reflected by different ratios of O radicals to O_2^+ ions and by ion energy. Ion bombardment in the presence of the O_2^+ ions decreases the plasma damage, although, in spite of the expectations, the damage reduction is not related to pore sealing. Analysis of the nature of the plasma damage reduction is the main purpose of this work.

II. EXPERIMENT

190 nm thick porous SiOCH layers were deposited on top of 300 mm Si wafers using PECVD. The low-*k* matrix material was deposited together with an organic porogen.²¹ Ultraviolet light ($\lambda = 172 \pm 30$ nm) assisted thermal curing was used to remove porogen and to cross-link the film skeleton. The resulting EP porosity was close to 33%, the *k*-value of the films was close to 2.3. A Lam 2300[®] Versys[®] Kiyo[®] chamber was used for plasma exposure. The chamber was equipped with the standard system for recording the optical emission spectrum. The top power is understood as the power delivered to TCP (inductively coupled) coil that powers the plasma above the wafer while the bottom power refers to the power delivered to the electrostatic chuck (ESC) (capacitively coupled) that carries the wafer (Fig. 1). Conditions are set to an arbitrary value of 10 mT, 100 SCCM

TABLE I. Etch rate as measured on a photoresist wafer is shown for the different conditions. Exposure times for the samples are chosen to equivalently remove 400 nm of photoresist.

Condition	Resist etch rate (nm/min)	Exposure time (s)	Equivalent resist removal (nm)
BPO	170	140	400
T&BP	375	64	400
TPO	120	200	400

(SCCM denotes cubic centimeter per minute at STP) O_2 , and 60 °C for chamber and ESC temperature. The major part of the experiments was carried out with 200 W top power and 240 W bottom power. Exposure times are set at an equivalent photoresist removal of 400 nm. Such normalization makes the results more practically valuable because the exposure time of low-*k* films depends on the resist strip rate.³ For all three of the plasma conditions, photoresist etch rates are determined and listed in Table I. One can see that the highest resist strip rate was observed in the T&BP condition (more than twice as large as in the BPO condition). The lowest resist strip rate corresponds to the TPO condition. The resist strip rate in the T&BP condition is larger than a simple superposition of BPO and TPO etch rates, which might suggest a change in the mechanism of the chemical reaction of the resist with oxygen in the presence of ion bombardment. However, more accurate quantitative analysis is needed for the evaluation of all key plasma components such as concentration of active radicals, concentration and energy of ions, etc. After the exposure, the samples are submitted to different analysis techniques. SE measurements are carried out to record the optical parameters of pristine and plasma modified low-*k* films. The spectra are taken in the wavelength range of 155–750 nm on an Aleris and for 240–780nm on an F5 spectroscopic ellipsometer from KLA Tencor. With knowledge of the characteristics of the pristine layer, a two layer model is applied to characterize the plasma modified layer by fitting. It was assumed that the bottom (nonmodified) layer has optical characteristics similar to the pristine layer. FTIR spectroscopy was carried out on a Thermo scientific FTIR 6700 in the range of 400–4400 cm^{-1} averaging to 64 scans with a resolution of 4 cm^{-1} . Cross-sectional TEM analysis is performed on focused ion beam prepared specimens in a Tecnai F30 system operated at 300 keV. To protect the surface during the specimen thinning an evaporated 150 nm thick Al layer is used. The chemical information in nanometer scale is obtained by acquiring Si, O, and C energy filtered images in EFTEM mode and TOF SIMS. The TOF SIMS data have been obtained using an IONTOF IV instrument in a noninterlaced dual beam mode with a Xe sputtering beam and a bunched 15 keV Ga analysis beam to detect negative secondary ions. The Ga analysis beam has been rastered over an $80 \times 80 \mu m^2$ area. The Xe beam has been used with 1 keV of impact energy using a raster size of $400 \times 400 \mu m^2$. A flood gun has been used to compensate the charge. Porosity, pore size distribution, and bulk hydrophilicity were measured by using ellipsometric porosimeter EP-10 equipped

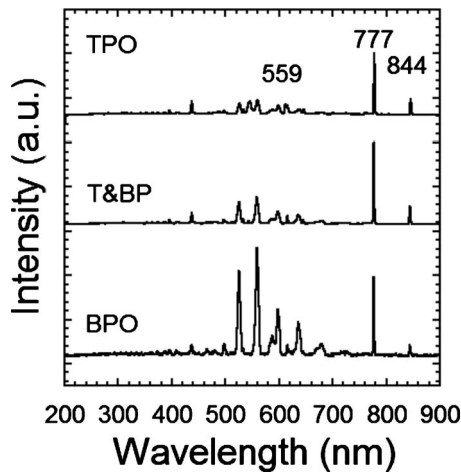


FIG. 2. Optical emission from the three plasma conditions as obtained from an oxide wafer. The relative intensities of the O_2^+ (559 nm) and the O (777 nm, 844 nm) emission change.

with SENTECH 801 spectroscopic ellipsometer ($\lambda = 350\text{--}850$ nm). The ellipsometer is mounted on a special vacuum chamber that can be filled with a solvent vapor (such as toluene or water) from special liquid sources in a controllable way.^{22,23} Toluene vapors are used for evaluation of open porosity because of its near zero contact angle with pristine and damaged low-*k* materials.²² Water based EP is used for characterization of internal hydrophilicity of the films. The amount of adsorbed water depends on the concentration of hydrophilic centers and, therefore, it is used as a measure of plasma damage.²³

III. RESULTS AND DISCUSSIONS

A. Plasma characterization

In order to shed some light on the plasma composition, the optical emission spectrum (OES) from the plasmas is recorded. Si wafers covered by SiO_2 films were used in these experiments because SiO_2 is not modified by oxygen plasma and, therefore, the impact of chemical reaction on plasma composition and characteristics is minimized. The OES spectra resulting from the three conditions (TPO, T&BP, and BPO) are shown in Fig. 2. The strongest emissions are due to either the oxygen atom (radical) (777, 844, and 615 nm) or the O_2^+ ion (559, 525, 597, 587, and 635 nm). The ratio of emission intensities of these two species is different for the three plasma conditions. While for the BPO condition the emission intensities of 777 nm radical line and the 559 O_2^+ are comparable, the 777 nm line becomes much stronger if the top power is switched on (T&BP condition). The difference increases going to a top power only based plasma (TPO condition). Relative to the O_2^+ (559nm) intensity, the radical intensity (777 nm and 844nm) increases by a factor of about 10 going from the BPO condition to the TPO condition via the T&BP, see Fig. 3.

It is necessary to mention that the correlation of the relative intensities with the ratio of oxygen radicals and ions is semiquantitative because it can be partially affected by a

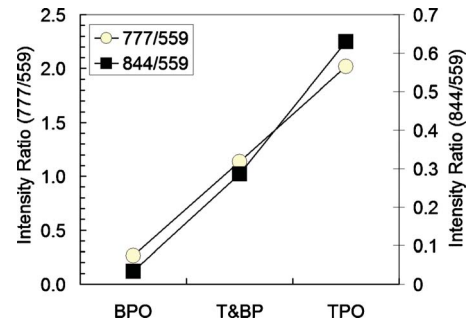


FIG. 3. (Color online) OES emission ratio of the O_2^+ (559nm) and the O (777 nm, 844 nm) emissions indicate a change in radical to ion ratio.

change in the electron energy distribution function (EEDF) in different exposure conditions.^{24,25} Optical emission intensities for both atoms and ions lines are a function of

$$I_{O,O_2^+} = \int_{\epsilon_{th}}^{\infty} \epsilon \sigma_{O,O_2^+}(\epsilon) f(\epsilon) d\epsilon,$$

where $\sigma_{O,O_2^+}(\epsilon)$ are excitation cross sections of emission states of atoms and ions, and $f(\epsilon)$ is EEDF with normalization condition $\int_0^{\infty} \epsilon^{1/2} f(\epsilon) d\epsilon = n_e$ (n_e is electron density). The EEDF in the TPO, T&BP, and BPO conditions can be quite different and, therefore, to compare, for instance, the concentration of O atoms generated in each condition, it is necessary to perform actinometry measurements. However, the observations presented in Figs. 2 and 3 are in line with the reasoning that adding top power generates oxygen radicals. If no top power is used (BPO), the plasma is capacitive coupled resulting in relatively more O_2^+ ions. Adding top power to the plasma increases the O/ O_2^+ ratio and lowers the energy of the bombarding ions that could result in a different modification of low-*k* film. In summary, going from BPO to T&BP and TPO the O/ O_2^+ ratio increases while the ion energy decreases.

B. Damage characterization by FTIR, WCA, and water EP

A first assessment of the plasma induced modifications was done by FTIR. The most pronounced change of FTIR spectra happens at 1275 cm^{-1} due to the CH_3 deformation bending in $CH_3\text{—Si}$ bonds.²⁶ These groups are introduced into low-*k* dielectrics to decrease the volume polarizability and provide hydrophobic properties and therefore, their removal is an important sign of plasma damage. The evolution of this absorbance under different conditions is shown in Fig. 4. All applied conditions cause a decrease in absorbance compared to the pristine film. In the case of applied bottom power, BPO, and T&BP, the decrease is only partial and reaches saturation while for the TPO conditions the peak completely vanishes indicating a complete modification of the low-*k* film. Additionally, the change in Si— CH_3 absorbance is quite similar for the BPO and T&BP (the final BPO absorbance remains a little stronger than the T&BP). There-

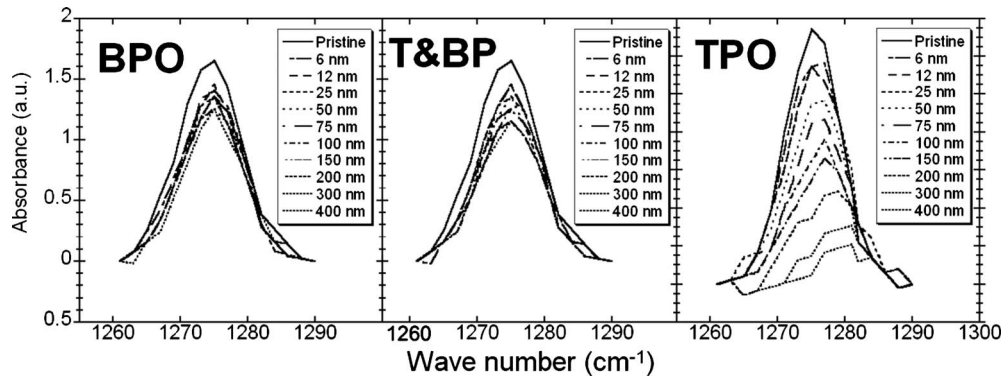


FIG. 4. (a) Change in FTIR absorbance at 1275 cm^{-1} after exposure in TPO, BPO, and T&BP conditions during the time necessary to remove certain amount of resist (legend). In the case of TPO the absorbance completely disappears, while for BPO and T&BP the absorbance partially remains.

fore, the highest hydrophilicity can be expected for the TPO exposed samples while the BPO and T&BP samples should be less hydrophilic.

Water contact angle and water-based EP measurements confirm these expectations. For the TPO condition a WCA of 0° corresponds to a high degree of surface hydrophilization. The BPO and T&BP have a WCA of 29.4° and 36.2° , respectively. Therefore, all low-*k* surfaces are significantly hydrophilic since for pristine material the WCA is equal to 95° . However, WCA shows only surface hydrophilization while the bulk hydrophilization depends on the depth of modification.

Internal (bulk) hydrophilicity of these films was measured by water-based EP. Gradual change in humidity from vacuum (10^{-4} Torr) up to 100% ($P/P_0=1$) in EP chamber allows to measure the amount of adsorbed water, which reflects the concentration of hydrophilic centers and the surface energy of pore wall.

EP analysis starts with the measurement of the initial optical characteristics of the films of interest (after plasma modification but before water adsorption). The results of such preliminary measurements are presented in Fig. 5(a) and Table II. The refractive index of the TPO sample before adsorption is equal to 1.33 at 632.8 nm, which is signifi-

cantly lower than the value measured for the pristine low-*k* film (1.37). The refractive index (RI) values for the films exposed in BPO and T&BP conditions are close to one another and slightly higher than the values obtained with pristine films (1.38–1.39 against 1.37). According to the Lorentz–Lorenz equation the RI is dependent on the porosity as well as on the composition. RI values for the relevant materials are as follows: air has a RI of 1, SiO_2 has a RI of 1.46, water has a RI of 1.33, while polymers display RI values of 1.5–1.6. Under vacuum conditions the RI increases because water adsorption is limited. Thus, under vacuum, the reduction to 1.33 for the TPO can be explained by an increase in porosity or the removal of the relative high RI organic compounds. On the other hand for the BPO and T&BP cases, organic material is removed but the RI remains 1.38–1.39, indicating a densification.

For estimating the thickness of the plasma damaged layer, spectra are recorded in air ambient and a two layer approach is used: a pristine layer at the bottom and damaged layer at the top. The thicknesses of both layers and the parameters of the damaged layer are fitted while the parameters for the pristine layer remain fixed. For the fitting of the pristine material, a three harmonic oscillators (HOs) model is sufficient for spectra down to 250 nm while six HOs are required for

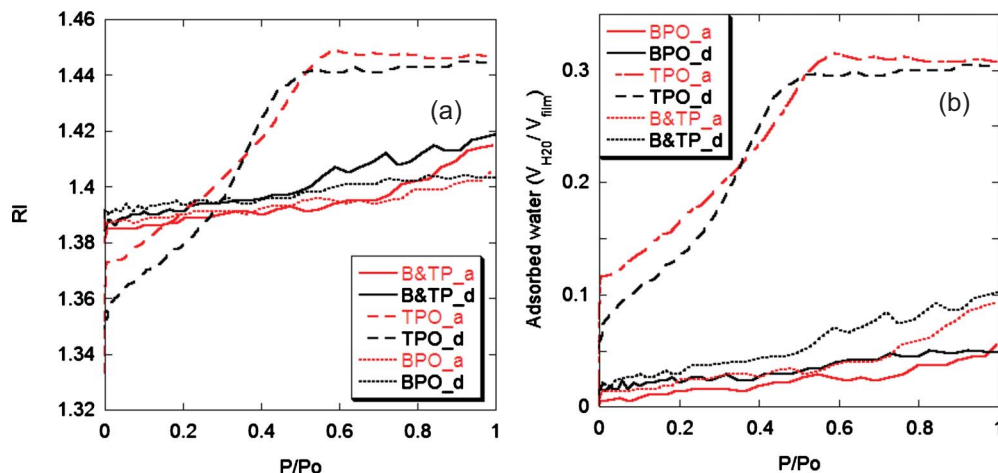


FIG. 5. (Color online) Change in refractive index (a) and amount of adsorbed water (b) during adsorption and desorption.

TABLE II. Properties as determined from ellipsometric spectroscopy and porosity are shown. Porosity after exposure is relatively close to the pristine value of 33%. No indication of sealing is found.

Condition	Photoresist removal (nm)	Initial thickness (nm)	Pristine thickness (nm)	Damaged thickness (nm)	RI at 633 vacuum	Porosity (%)	Pore radius (nm)
Pristine	1.37	33	0.7
BPO	400	193	139	35	1.38	26	0.6
T&BP	400	193	121	49	1.38	28	0.7
TPO	400	180	0	136	1.33	35	0.7

simulating spectra down to 155 nm. A reasonable fitting of the damaged layer is achieved using one HO. The outcome for the three conditions with an equivalent photoresist removal of 400 nm is shown in Table II. In all cases shrinkage is observed which is the largest for the TPO condition where the layer is completely damaged. The BPO and the T&BP conditions show a partially damaged layer which is thickest for the T&BP.

Figure 5(b) presents the results of the recalculation of refractive indices to the amount of adsorbed water as described in elsewhere.²³ The amount of adsorbed (condensed) water after TPO exposure is close to the open porosity of pristine films (as measured by toluene based EP: see below), which suggests complete hydrophilization of the low-*k* material (all pores are completely filled by water). The water amount adsorbed in a BPO film is about 5%, which is close to the one for pristine low-*k* materials. T&BP sample showed hydrophilicity close to 10%, which is still three times lower than the film porosity but twice as high as for the BPO sample. The data obtained by water EP show very good consistency with the carbon depletion observed by FTIR.

The described phenomena should be reflected by depth profile of CH₃ concentration. The depth profile of CH₃ concentration and gradient of density were analyzed by using TOF SIMS and EFTEM. This information will be analyzed in Secs. IIIC–IIIE.

C. EFTEM and TOFSIMS: Gradient of chemical composition

The elemental composition and its gradients in the damaged low-*k* materials are investigated by EFTEM and TOF SIMS. For EFTEM, the samples are prepared with an Al cover layer. The total thickness of the layers, as measured by EFTEM, is slightly lower than the values obtained by SE, which we attribute to shrinking of the layers during sample preparation. Figure 6 shows the EFTEM mappings for silicon (Si), carbon (C), and oxygen (O) after exposure during the time necessary for removal of 400 nm thick photoresist (Table I). A brighter area corresponds to a higher concentration of the targeted species. Silicon is rather uniformly distributed in the TPO sample while for BPO and T&BP conditions, the silicon map is brighter at the top of the sample. Since shrinking is observed and given the fact that oxygen does not form a volatile compound with silicon, a higher Si concentration is expected at the top surface. In regular TEM

these surface layers of the BPO and T&BP samples show a little darkening compared to the bulk indicating a densification. Looking at the carbon maps, the TPO sample is completely carbon depleted and shows a speckled pattern that is not understood. In the case where bottom power is applied, only the top surface is carbon depleted. A similar behavior is observed for the oxygen maps: complete oxidation for the TPO condition and higher oxygen content for the BPO and the T&BP condition near the surface. The surface layers as estimated from TEM, in the case of BPO and T&BP conditions, have thicknesses of 20 and 24 nm, respectively, and they are in reasonable agreement with the SE results (35 and 49 nm, respectively). As mentioned above, these wafers were exposed during the time necessary for removal of 400 nm thick photoresist. Thickness of the damaged layer versus non-normalized (absolute) exposure time as obtained from SE is presented in Fig. 7. One can see that all of them have a tendency to saturation but it happens at a different time and

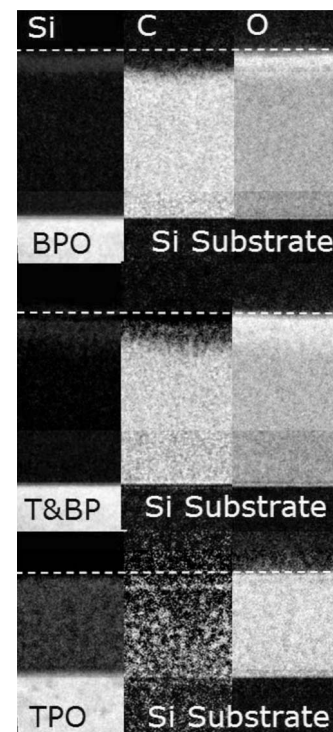


FIG. 6. EFTEM elemental (Si, C, and O) profiles of low-*k* samples exposed in BPO, T&BP, and TPO conditions are shown.

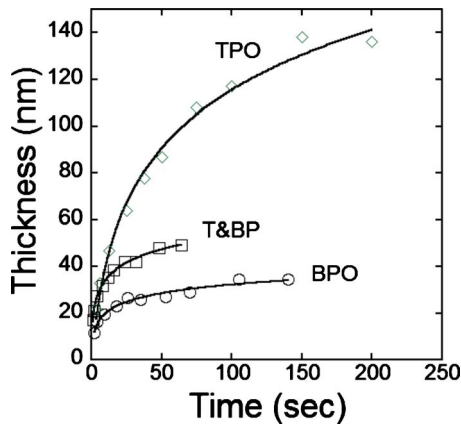


FIG. 7. (Color online) Time evolution of damaged layer as estimated by SE for the BPO, T&BP, and BPO plasma condition.

correspond to different damage depth. The depth of damage is highest for the TPO condition, followed by T&BP and BPO, respectively.

TOF SIMS data are shown in Fig. 8. Up to about 5 nm depth, the signal is difficult to interpret because of surface contamination (<1 nm) and its transient nature (5 nm). From 5 nm depth onward, following the oxygen signal of the TPO condition, a constant yield is observed confirming a uniform oxygen distribution throughout the sample. The profile of oxygen concentration in BPO and T&BP conditions is like a mirror image of the carbon and hydrogen concentration. The reason is that the carbon depletion increases the relative oxygen concentration on the top part of the films (the films become more SiO₂-like). The degree of carbon depletion is higher than the degree of hydrogen depletion. In both these cases, the hydrogen and carbon profiles are similar for both BPO and T&BP. However, the profiles become different starting from 20 nm depth: The region of the H and C depletion is more deeply extended into the film in the case of T&BP conditions.

As expected, the degree of carbon and hydrogen depletion is the highest in the TPO case. For the TPO condition, the carbon and hydrogen concentrations are two and one order of magnitude, respectively, lower than the levels in a pristine film (compared to the bulk C and H concentration in Fig. 8). It is surprising that the C and H concentrations are higher on the top part (5–15 nm depth) of the films. The region of C and H enrichment is higher than the ones observed in BPO and T&BP samples in this region. A possible explanation is condensation of by-products of carbon compounds reaction with oxygen. A similar observation and conclusion were reported in the paper by Braginsky *et al.*¹⁷ where plasma damage of the same low-*k* material was studied using a specially designed plasma system.

The constant oxygen signal in the TPO sample indicates a uniform matrix and therefore, the carbon and hydrogen signals are representative for the concentration. The bright oxygen region from the BPO and T&BP samples have depths of 35 and 45 nm, respectively, and have the same intensity as the TPO signal. It indicates that the oxygen is located in a

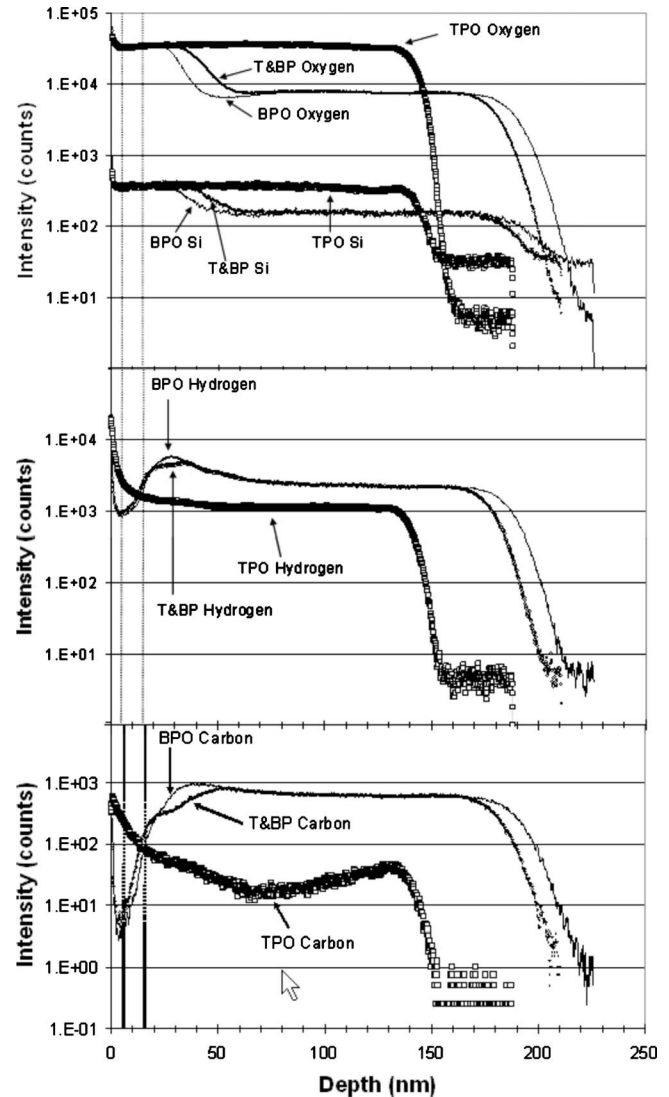


FIG. 8. TOF SIMS data. The oxygen, carbon, hydrogen, and silicon signal for the three samples as function of depth.

similar matrix and has similar concentration. The oxygen signal in the TPO sample remains constant until the substrate is reached suggesting complete damage of low-*k* film.

The silicon signal behaves in the same way. For all of the samples, the same Si intensity is observed on the top layer while for the samples with bottom power a drop is observed. For the T&BP, the drop occurs at 35 nm depth while for the BPO it is visible at 45 nm. The observed Si yield drop (over half an order of magnitude) corresponds to the transition from oxidized to pristine material. The fact that the silicon yield drops again when reaching the silicon substrate illustrates once more the impact of entering a different matrix. The surrounding matrix impacts the ionization yield during ion impact making it hard to convert intensities to concentration. A lower Si intensity does not necessarily mean a lower Si concentration. In short, the two layer model is found back in the oxygen and silicon TOF SIMS data. Furthermore, compared to the BPO sample, the hydrogen and carbon signals from the T&BP show a fine structure in the

top layer. At around a depth of 20 nm, the signals for the BPO and the T&BP split up: The signal for the BPO condition continues to increase at the same rate while the signal increase slows down for the T&BP resulting in a deeper damage from 20 nm onward.

In conclusion, the EFTEM and TOF SIMS results confirm that applying bottom power leads to formation of compositional gradient while the TPO condition modifies the complete sample. Again, the modified top layer of the T&BP consists of two layers itself. Down to a depth of 20 nm BPO and T&BP have the same hydrogen and oxygen profiles. Between 20 nm depth and the region of the unaffected area, the profiles differ until they merge again at the pristine interface.

D. EP

The presented results show that low-*k* films treated in BPO and T&BP conditions show limited plasma damage in comparison with the films treated in TPO condition. The reduction in plasma damage during the plasma exposure when the substrate is biased has already been observed and it has been a subject of quite extensive discussions in literature.^{1,2,27–31} The most common point of view is that the pores can be sealed because of ion induced densification of the surface layer. However, it was shown that this scenario might be limited to microporous materials only.^{27,28} Recent attempts to separate the contribution of different plasma components demonstrated the complicated nature of this phenomena.^{16–18} For instance, a quite efficient sealing of pores in some cases can be achieved by combined effects of chemical, photochemical, and ion stimulated processes.^{32,33} Some authors^{27,28} reported that the plasma damage reduction can be related to removal of the degraded layer by the oxygen ions due to the high chemical sputtering rate. However, this assumption is not confirmed by a recent research that showed no significant role of ion bombardment.²⁹ Therefore, evaluation of the pores accessibility and pore size is an extremely important step in research oriented toward understanding plasma damage reduction.

Porosity and pore size of these films were studied using ellipsometric porosimetry, which is known as an efficient method for this purpose.² Figure 9 shows the toluene adsorption/desorption isotherms for the three samples. The TPO sample showed the highest porosity but the value does not differ from the pristine samples (35% and 33% of porosity), Table II. A change in refractive index from 1.37 (pristine) to 1.33 (damaged) should correspond to much higher change in porosity. The seeming contradiction between increasing porosity and refractive index suggests that the reduction in refractive index was most probably related to removal of carbon containing compounds (residues) that have a high refractive index.³⁴

The BPO and the T&BP samples display lower open porosity values of 26% and 29%, respectively. The lower open porosity in these samples can be explained by the fact that certain parts of micropores became inaccessible for the toluene adsorption (partial sealing). In our case, the surface densification is very limited, which is reflected by the small

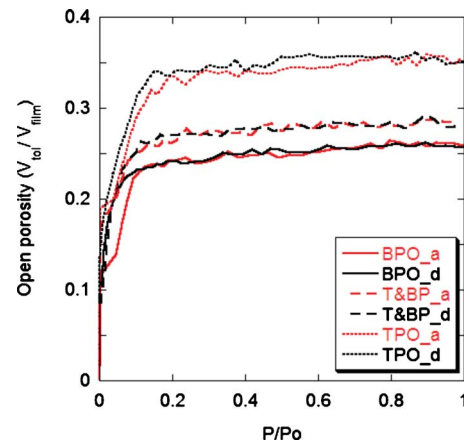


FIG. 9. (Color online) Toluene vapor adsorption isotherms during adsorption and desorption.

increase in the refractive index. Additional proof of the limited surface densification is obtained from the calculated pore size distribution (Fig. 10). No change in pore size distribution was observed in all three experimental conditions. Basically, Figs. 5, 9, and 10 show a limited densification while molecules such as toluene and water that are larger than an oxygen radical can still easily penetrate into the low-*k*. Therefore, similar to that of Posseme *et al.*,²⁹ we can conclude that the densification induced by ion irradiation does not play an important role in the studied case with respect to plasma damage.

E. Factors reducing the plasma damage

The presented data can be summarized as following:

- The TPO condition drastically reduces the concentration of Si—CH₃ bonds through the film, while the degree of carbon depletion in T&BP and BPO conditions is much smaller. Note that the principle difference in BPO and T&BP conditions in comparison with TPO is the higher ion energy and the higher O₂⁺/O ratio.

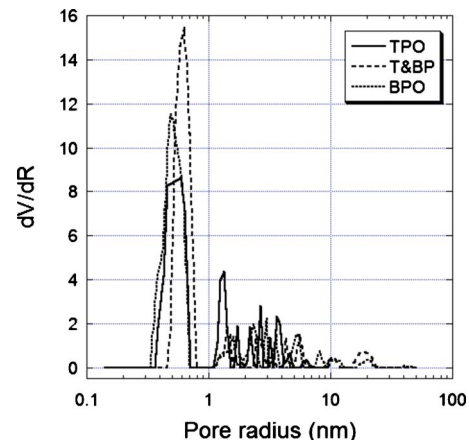


FIG. 10. (Color online) Pore size distribution after exposure to the three conditions TPO, T&BP, and BPO.

- The rate of carbon depletion is nonlinear and has a tendency to saturation. The smallest saturation level (lowest depth of plasma damage) corresponds to the BPO condition, the largest one to TPO. The depth of carbon depletion (EFTEM, TOF SIMS) is consistent with degree of hydrophilization (EP).
- The films exposed in the TPO condition have, compared to the pristine one, similar porosity but lower refractive index. However, the change in the refractive index is not completely consistent with the large change in porosity. This disagreement is probably related to the ability of an O₂-plasma to remove not only Si—CH₃ groups but also other carbon containing compounds that have a large refractive index (porogen residue).³⁴
- An increase in refractive index and a change in porosity of the films exposed in BPO and T&BP conditions are very small. These facts together with unchanged pore size suggest that the low plasma damage is not related to surface sealing.

Using these facts, the nature of this plasma damage reduction may be analyzed. The depth of damage is related to the penetration depth of oxygen radicals. The pore size in these films is much smaller than the mean free path length of atoms and molecules in a plasma, and therefore the penetration of active radicals is described by the random walk theory. According to this theory, the depth of penetration is defined by¹²

$$L_{\text{pen}} \sim adN_{\text{rec}}^{0.5}$$

where a is dimensionless and relates the pore diameter d to the typical distance between two collisions, and N_{rec} is the average number of collisions needed for recombination. Zero penetration depth can be provided by complete pore sealing ($d=0$). However, in our case almost no change in pore size is observed. Therefore, the reduction in the depth of O atoms penetration can only be defined by their recombination probability $\gamma_{\text{O}}=1/N_{\text{rec}}$. The recombination probability of oxygen radicals in this film without preliminary plasma modification was found to be 6.5×10^{-3} .¹²

An estimation of the penetration depth of oxygen radicals can be obtained by assuming that the typical distance between the two collisions of an O atom with the pore wall (a) is about 1.5 times the pore diameter. Therefore the penetration depth of oxygen radicals in a nonmodified low- k film is equal to 27 nm, which is quite close to depth of damage after BPO exposure condition. Using the same equation, we can find that the depth of penetration for oxygen radicals after the TPO condition should correspond to $\gamma_{\text{O}}=(3-4) \times 10^{-4}$, which is very close to the reported values of oxygen atoms recombination on a silica surface.³⁵ The TPO condition generates a high concentration of oxygen radicals that results in a relatively fast removal of the carbon containing groups. The resulting surface of the pore wall becomes similar to the surface of SiO₂ that has a low probability of recombination for oxygen atoms.³⁶

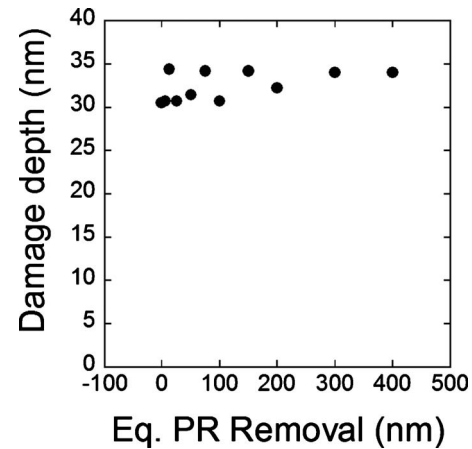


FIG. 11. Thickness of the oxidized layer as estimated by SE. A TPO condition is applied for various times after a BPO condition. The thickness of the damaged layer remains constant.

The recombination probability can be increased by the generation of surface active centers. In both the Langmuir–Hinshelwood and Eley–Riedel mechanisms of recombination, these centers should be able to form sufficiently strong chemical bonds with oxygen atoms.^{36,37} In the case of a silica surface, such centers are generated by exposure in a plasma.³⁷ The mechanism of the generation of active centers by a reactive plasma has been intensively discussed in literature.^{37–41} Although the mechanism of the generation of such centers can be different, it was proposed that the active sites might be related to electron deficient or deformed siloxane bridges.⁴¹ Surface contamination may also play an important role⁴² but it is difficult to expect that the contamination level can drastically change in the conditions of our study. Relatively large values¹² (in comparison with silica) in pristine low- k films are generally consistent with the assumption about the important role of electron deficient siloxane bridges and deformed siloxane bridges. Introduction of C-containing hydrophobic groups changes the electronic condition and structure of siloxane bridges. The possibility of reduction in plasma damage by increasing of the concentration of hydrophobic groups supports this conclusion.¹⁰

An additional interesting fact is that the degree of plasma damage is still quite O₂⁺ small in the T&BP condition and close to that of the BPO condition. It is known that switching on the top power drastically increases the degree of dissociation. A reasonable explanation is that the energetic O₂⁺ ions are extremely efficient at generating active centers in the low- k film and that these centers have a sufficiently long lifetime. To prove it, special experiments were carried out. The low- k films were exposed in a BPO plasma and then exposed to the TPO conditions. Wafers are exposed to a two-step plasma treatment: first the BPO condition for an equivalent photoresist removal of 400 nm followed by the TPO condition for various times. Because of the open porosity that is expected, the radicals can easily penetrate and damage the low- k deeper. Figure 11 shows that the opposite is found, the depth of damage remains equal to the value of about 35 nm found after BPO condition. It is found that films that

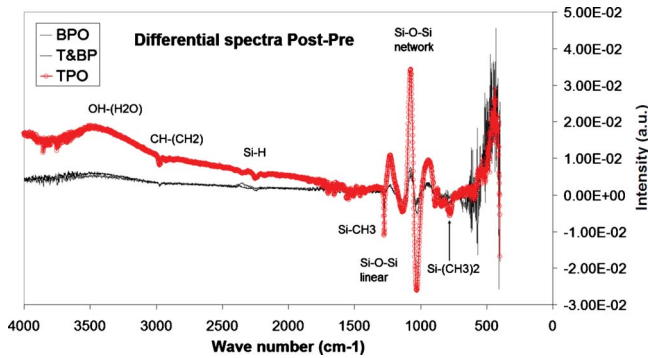


FIG. 12. (Color online) Differential FTIR spectra for the BPO, T&BP, and TPO conditions. The TPO shows next to the reduction in CH groups a Si—O—Si bound reconstruction from linear to a network type of structure.

were preliminary exposed under BPO conditions are not damaged further under TPO condition, even after long exposure time (Fig. 11). These experiments support our conclusion related to the efficiency of the generation of active centers by O_2^+ ions and that these centers have quite a long lifetime.

An insight into the nature of active centers can be obtained from the comparison of differential FTIR spectra of the studied films (Fig. 12). In this figure, FTIR spectrum of pristine film was subtracted from the spectra measured after exposure to TPO, BPO, and T&BP conditions. In addition to the expected high concentration of adsorbed water, the TPO sample shows stronger decrease in C—H(CH₂), Si—H, SiCH₃, and Si(CH₃)₂ concentrations and huge reconstruction of Si—O—Si groups. The principal difference for the TPO sample is that most of the linear (large angle, and suboxide) Si—O—Si groups were reconfigured into SiO₂ network groups that have a tetrahedral structure. This is the reason why the recombination coefficient of oxygen atoms in completely damaged low-*k* films is becoming typical for pure silica [$\gamma_0 = (3-4) \times 10^{-4}$] while this value for nondamaged low-*k* films is about an order of magnitude larger (6.5×10^{-3}). The most obvious way to reach a high concentration of the groups with linear structure is to keep a relatively high concentration of methyl groups bonded to Si atoms instead of oxygen like $=O_2=Si-CH_3$ and/or $=O_2=Si-(CH_3)_2$. This is the reason why the degree of plasma damage decreases with increasing carbon concentration.¹⁰ In some cases a high carbon concentration is desirable because of the higher possibility of changing their properties during the resist strip.³⁴ Therefore, it is important to find a way to increase concentration of recombination centers that do not directly depend on carbon concentration. It seems that ion irradiation can modify the SiO₂ surface and create such centers.³⁵⁻³⁹ However, application of these phenomena to low-*k* dielectrics needs additional research.

IV. CONCLUSIONS

Plasma damage of SiCOH low-*k* films in oxygen plasmas is studied using a transformer coupled plasma reactor. The concentration of oxygen atoms and energetic O_2^+ ions is var-

ied by using three different plasma conditions: (1) bottom power only, (2) bottom and top power simultaneously, and (3) top power only. It is shown that the TPO condition generates the plasma with the highest ratio of radicals/ions concentrations. After plasma exposure, the low-*k* samples were characterized by various advanced experimental techniques. It is shown that the ion bombardment induced by the bottom power minimizes the plasma damage by increasing the recombination coefficient of oxygen radicals. Contrary to the expectations, densification of the top surface by ion radiation was negligible. It is concluded that the increase of the recombination coefficient is mainly provided by the modification of the pore wall surface and the creation of chemically active centers that stimulate the recombination of oxygen atoms. The most probable active centers are electron deficient siloxane bridges and deformed siloxane bridges. The results show a principal possibility for the reduction in plasma damage without sealing of low-*k* top surface. This is an important conclusion because, in general, any sealing increases the *k*-value.

- ¹K. Maex, M. R. Baklanov, D. Shamiryan, F. Iacopi, S. H. Brongersma, and Z. S. Yanovitskaya, *J. Appl. Phys.* **93**, 8793 (2003).
- ²D. Shamiryan, M. R. Baklanov, S. Vanhaelemeersch, and K. Maex, *J. Vac. Sci. Technol. A* **20**, 1923 (2002).
- ³J. Bao, H. Shi, J. Liu, H. Huang, P. S. Ho, M. D. Goodner, M. Moinpour, and G. M. Kloster, *J. Vac. Sci. Technol. B* **26**, 219 (2008).
- ⁴H. Shi *et al.*, *Appl. Phys. Lett.* **93**, 192909 (2008).
- ⁵M. A. Worsley, S. F. Bent, S. M. Gates, N. C. M. Fuller, W. Volksen, M. Steen, and T. Dalton, *J. Vac. Sci. Technol. B* **23**, 395 (2005).
- ⁶R. J. O. M. Hoofman, G. J. A. M. Verheijden, J. Michelon, F. Iacopi, Y. Travaly, M. R. Baklanov, Zs. Tokei, and G. Beyer, *Microelectron. Eng.* **80**, 337 (2005).
- ⁷X. Hua *et al.*, *J. Vac. Sci. Technol. B* **24**, 1238 (2006).
- ⁸A. Grill and V. Patel, *J. Electrochem. Soc.* **153**, F169 (2006).
- ⁹M. Chaudhari, J. Du, S. Behera, S. Manandhar, S. Gaddam, and J. Kelber, *Appl. Phys. Lett.* **94**, 204102 (2009).
- ¹⁰E. T. Ryan *et al.*, *J. Appl. Phys.* **104**, 094109 (2008).
- ¹¹M. R. Baklanov, A. Urbanowicz, G. Mannaert, and S. Vanhaelemeersch, Proceedings of the Eighth International Conference on Solid-State and Integrated Circuit Technology (ICSST), 2006 (unpublished), p. 291.
- ¹²T. V. Rakhimova *et al.*, *Advances in Plasma Processing for Semiconductor Manufacturing*, special issue of *IEEE Trans. Plasma Sci.* **37**(9), 1697 (2009).
- ¹³G. Mannaert, M. R. Baklanov, Q. T. Le, Y. Travaly, W. Boullart, S. Vanhaelemeersch, and A. M. Jonas, *J. Vac. Sci. Technol. B* **23**, 2198 (2005).
- ¹⁴A. Furuya, E. Soda, M. Shimada, and S. Ogawa, *Jpn. J. Appl. Phys., Part 1* **44**, 7430 (2005).
- ¹⁵S. Uchida, S. Takashima, M. Hori, M. Fukasawa, K. Ohshima, K. Nagahata, and T. Tatsumi, *J. Appl. Phys.* **103**, 073303 (2008).
- ¹⁶H. Shi *et al.*, *IEEE International Interconnect Technology Conference in 2009*, Sapporo, 2009 (unpublished).
- ¹⁷O. V. Braginsky *et al.*, *Mater. Res. Soc. Symp. Proc.* **1156**, D01 (2009).
- ¹⁸V. V. Smirnov, A. V. Stengach, K. G. Gaynullin, V. A. Pavlovsky, S. Rauf, and P. L. G. Ventzek, *J. Appl. Phys.* **101**, 053307 (2007).
- ¹⁹F. Iacopi, Y. Travaly, M. Van Hove, A. M. Jonas, J. M. Molina-Aldareguia, M. R. Elizalde, and I. Ocana, *J. Mater. Res.* **21**, 3161 (2006).
- ²⁰Y. Li *et al.*, *J. Appl. Phys.* **104**, 034113 (2008).
- ²¹P. Verdonck *et al.*, *Surf. Coat. Technol.* **201**, 9264 (2007).
- ²²M. R. Baklanov, K. P. Mogilnikov, V. G. Polovinkin, and F. N. Dultsev, *J. Vac. Sci. Technol. B* **18**, 1385 (2000).
- ²³M. R. Baklanov, K. P. Mogilnikov, and Q. T. Le, *Microelectron. Eng.* **83**, 2287 (2006).
- ²⁴E. Kunnen, T. V. Rakhimova, D. Shamiryan, H. Struyf, W. Boullart, and M. R. Baklanov, *Microelectron. Eng.* **87**(3), 462 (2010).
- ²⁵N. C. M. Fuller, M. V. Malyshev, V. M. Donnelly, and Irving P. Herman,

- Plasma Sources Sci. Technol. **9**, 116 (2000).
- ²⁶K. Y. Yiang and W. J. Yoo, *J. Vac. Sci. Technol. B* **23**, 433 (2005).
- ²⁷S. W. Hwang, G. R. Lee, J. H. Min, and S. H. Moon, *Surf. Coat. Technol.* **174–175**, 835 (2003).
- ²⁸E. Kondoh, T. Asano, A. Nakashima, and M. Komatu, *J. Vac. Sci. Technol. B* **18**, 1276 (2000).
- ²⁹N. Posseme, T. Chevolleau, T. David, M. Darnon, O. Louveau, and O. Joubert, *J. Vac. Sci. Technol. B* **25**, 1928 (2007).
- ³⁰T. Abell and K. Maex, *Microelectron. Eng.* **76**, 16 (2004).
- ³¹L. L. Chapelon, V. Arnal, M. Broekaart, L. G. Gosset, J. Vitiello, and J. Torres, *Microelectron. Eng.* **76**, 1 (2004).
- ³²A. M. Urbanowicz, M. R. Baklanov, J. Heijlen, Y. Travaly, and A. Cockburn, *Electrochem. Solid-State Lett.* **10**, G76 (2007).
- ³³H.-G. Peng *et al.*, *J. Electrochem. Soc.* **154**, G85 (2007).
- ³⁴A. M. Urbanowicz, K. Vanstreels, D. Shamiryan, S. De Gendt, and M. R. Baklanov, *Electrochem. Solid-State Lett.* **12**, H292 (2009).
- ³⁵G. Cartry, L. Magne, and G. Cernogora, *J. Phys. D: Appl. Phys.* **32**, L53 (1999).
- ³⁶G. Cartry, X. Duten, and A. Rousseau, *Plasma Sources Sci. Technol.* **15**, 479 (2006).
- ³⁷L. Magne, H. Coitout, G. Cernogora, and G. Gousset, *J. Phys. III* **3**, 1871 (1993).
- ³⁸J. Jolly and J.-P. Booth, *J. Appl. Phys.* **97**, 103305 (2005).
- ³⁹A. Rousseau, G. Cartry, and X. Duten, *J. Appl. Phys.* **89**, 2074 (2001).
- ⁴⁰N. V. Mantzaris, E. Gogolides, A. G. Boudouvis, A. Rhallabi, and G. Turban, *J. Appl. Phys.* **79**, 3718 (1996).
- ⁴¹J. Perrin, M. Shiratani, P. Kae-Nune, H. Videlot, J. Jolly, and J. Guillon, *J. Vac. Sci. Technol. A* **16**, 278 (1998).
- ⁴²J. Guha, R. Khare, L. Stafford, V. M. Donnelly, S. Sirard, and E. A. Hudson, *J. Appl. Phys.* **105**, 113309 (2009).